ACCELERATED PUBLICATION

TIRF imaging of docking and fusion of single insulin granule motion in primary rat pancreatic β-cells: different behaviour of granule motion between normal and Goto–Kakizaki diabetic rat β-cells

Mica OHARA-IMAIZUMI, Chiyono NISHIWAKI, Toshiteru KIKUTA, Shintaro NAGAI, Yoko NAKAMICHI and Shinya NAGAMATSU[1]

Department of Biochemistry (II), Kyorin University School of Medicine, Shinkawa 6-20-2, Mitaka, Tokyo 181-8611, Japan

We imaged and analysed the motion of single insulin secretory granules near the plasma membrane in live pancreatic β-cells, from normal and diabetic Goto–Kakizaki (GK) rats, using total internal reflection fluorescence microscopy (TIRFM). In normal rat primary β-cells, the granules that were fusing during the first phase originate from previously docked granules, and those during the second phase originate from 'newcomers'. In diabetic GK rat β-cells, the number of fusion events from previously docked granules were markedly reduced, and, in contrast, the fusion from newcomers was still preserved. The dynamic change in the number of docked insulin granules showed that, in GK rat β-cells, the total number of docked insulin granules was markedly decreased to 35 % of the initial number after glucose stimulation. Immunohistochemistry with anti-insulin antibody observed by TIRFM showed that GK rat β-cells had a marked decline of endogenous insulin granules docked to the plasma membrane. Thus our results indicate that the decreased number of docked insulin granules accounts for the impaired insulin release during the first phase of insulin release in diabetic GK rat β-cells.

Key words: diabetes mellitus, exocytosis, insulin release, membrane fusion, pancreatic β-cell, total internal reflection fluorescence microscopy (TIRFM).

INTRODUCTION

Imaging techniques are powerful tools for detecting vesicle trafficking in live cells and they have provided significant advances in understanding the mechanism of exocytosis [1–3]. In particular, the use of total internal reflection fluorescence microscopy (TIRFM; also called evanescent wave microscopy), which allows fluorescence excitation within a closely restricted domain close to the plasma membrane (within 100 nm) [4], has permitted us to observe single insulin granules undergoing exocytosis. We have previously reported a new approach that uses a GFP (green fluorescent protein)-tagged insulin granule system combined with TIRFM using insulinoma MIN6 cells [5], which allowed us to observe the docking and fusion of a single insulin granule with a high degree of time resolution. Nevertheless, TIRF imaging using primary β-cells was required to examine the altered exocytosis in diabetic β-cells, because the use of an animal model of disease is essential to reveal the pathophysiology.

In Type II diabetes, the impaired insulin release in the pancreatic β-cells when stimulated by glucose is well established [6]; in particular, the β-cell defect in Type II diabetes is characterized by a lack of first-phase insulin release in response to glucose stimulation [7,8]. Although the precise molecular mechanism of insulin release has yet been determined, it is generally accepted that the ATP-sensitive K^+ channels play a central role in insulin release [9,10]. Because the electrophysiological properties of the ATP sensitivity of the ATP-sensitive K^+ channels are not altered in the β-cells in diabetic animal models [11,12], impairments of the glucose metabolism may be involved in the defect in insulin release. Indeed, there are several reports that have shown that abnormal glucose metabolism in diabetic β-cells contributes to a failure in insulin release [13–16].

On the other hand, the fundamental components of the secretory machinery required for the docking and fusion of vesicles in neuronal cells [17] are also expressed in pancreatic β-cells [18,19]. We [20] and others [21,22] have demonstrated that the expression of the insulin exocytosis machinery, such as SNARE (soluble *N*-ethylmaleimide-sensitive fusion protein attachment protein receptor) proteins, is impaired in diabetic Goto–Kakizaki (GK) rat islets. Therefore, it is conceivable that there must be impairments in the insulin exocytotic process in diabetic β-cells; however, so far there has been no direct evidence to show that the final step of insulin exocytosis is impaired in diabetic β-cells, because of the limited methodologies previously available.

In the present study, we obtained high-resolved images of primary rat β-cells using a TIRF imaging system, which allowed us to explore the impaired docking and fusion status of insulin granules in live diabetic GK rat β-cells.

EXPERIMENTAL

Cells

Diabetic GK rats and non-diabetic male Wistar rats were obtained from a commercial breeder (Oriental Yeast, Tokyo, Japan). The rats were given free access to food and water until the start of experiments, which were conducted with 10-week-old male rats. The body weight of GK rats was not statistically different from that of controls. The plasma glucose concentration in the fed state, measured by the glucose-oxidase method with a glucose analyser (Toecho Super, Kyoto Daiichi Kagaku, Kyoto, Japan), was 222 ± 14 mg/dl ($n = 16$) in GK rats and 104 ± 11 mg/dl ($n = 18$) in control rats respectively ($P < 0.0001$). Pancreatic islets of Langerhans were isolated by collagenase digestion [20], with

Abbreviations used: FBS, fetal bovine serum; GFP, green fluorescent protein; eGFP, enhanced GFP; GK, Goto–Kakizaki; KRB, Krebs–Ringer buffer; RRP, readily-releasable pool; TIRF, total internal reflection fluorescence; TIRFM, TIRF microscopy.

[1] To whom correspondence should be addressed (e-mail shinya@kyorin-u.ac.jp).

some modification. Isolated islets were dissociated into single cells by incubation in Ca^{2+}-free Krebs–Ringer buffer (KRB) containing 1 mM EGTA, and cultured on fibronectin-coated (Koken Co., Tokyo, Japan) high-refractive-index glass coverslip (Olympus) in RPMI 1640 medium (Gibco BRL), supplemented with 10 % FBS (fetal bovine serum) (Gibco BRL), 200 units/ml penicillin and 200 μg/ml streptomycin at 37 °C, in an atmosphere of 95 % air/5 % CO_2.

Constructs and expression

Insulin-eGFP (enhanced GFP) cDNA expression vector was constructed in two steps. Human pre-proinsulin cDNA pchi 1–19 (provided by Professor G. I. Bell, Department of Biochemistry and Molecular Biology, University of Chicago, Chicago, IL, U.S.A.) lacking a TGA stop codon was amplified by PCR using forward primer, 5′-*GAATTC*CGGGGGTCCTTCTGCCATG-3′ (*Eco*R1 site is italicized), and reverse primer, 5′-*GGATCC*-CAGTTGCAGTAGTTCTCCAGC-3′, where TGA was replaced by TGG. The product was subcloned into a pGEM^{T}easy vector (Promega). The approx. 0.3 kb insulin cDNA fragment lacking stop codon was cleaved by *Eco*R1 and *Bam*H1 double digestion, which was subcloned into the *Eco*R1 and *Bam*H1 site of multiple cloning sites of pEGFP-N1 (Clontech/BD Biosciences, Palo alto, CA, U.S.A.). For the recombinant adenovirus production of insulin–GFP, a cDNA fragment containing pre-proinsulin and GFP was cut by *Eco*R1 and *Not*I restriction enzymes, which was ligated into the pAdex1CA cosmid vector, and Adex1CA insulin-GFP was prepared and amplified by the standard protocol (Takara Shuzo Co., Kyoto, Japan) as described previously [23]. The reverse primer used here encodes the C-terminus of pre-proinsulin, ending LENYCNWD. The fusion with the N-terminus of eGFP includes a short linker (provided by the pEGFP-N1 plasmid) such that the sequence reads LENYCNWDPPVATM (the linker sequence is underlined and M is the first residue of eGFP). Thus the junction between the C-terminus of pre-proinsulin and eGFP is different to that used in a previously reported construct [24]; this difference may account for the differential trafficking of the two constructs. For the infection of the pancreatic β-cells with the recombinant adenovirus, cultured single cells were incubated with RPMI 1640 medium (5 % FBS) and the required adenovirus (Adex1CA insulin-GFP: 30 multiplicity of infection per cell) for 1 h at 37 °C, after which RPMI 1640 medium with 10 % FBS was added. In normal primary β-cells infected with Adex1CA insulin-GFP, GFP-tagged insulin co-localized with IAPP (islet amyloid polypeptide) (results not shown), a marker for the insulin-containing large dense core granule [5], which indicated that GFP-tagged insulin was correctly sorted into the insulin secretory granules.

TIRFM

The Olympus total internal reflection system was used with minor modifications. Light from an Ar laser (488 nm) or an He/Ne laser (543 nm) was introduced into an inverted epifluorescence microscope (IX70, Olympus) through a single-mode fibre and two illumination lenses; the light was focused at the back focal plane of a high-aperture objective lens (Apo 100 × OHR; NA 1.65, Olympus). To observe GFP, we used a 488-nm laser line for excitation and a 515-nm long-pass filter for the barrier. To observe the fluorescence image of Cy3, we used a 543-nm laser line and a long-pass 590-nm filter. The infected cells on the glass coverslip (Olympus) were mounted in an open chamber and incubated for 30 min at 37 °C in KRB containing 110 mM NaCl, 4.4 mM KCl, 1.45 mM KH_2PO_4, 1.2 mM $MgSO_4$, 2.3 mM calcium gluconate, 4.8 mM $NaHCO_3$, 2.2 mM glucose, 10 mM Hepes (pH 7.4) and 0.3 % BSA. Cells were then transferred onto the thermostat-controlled stage (37 °C). Stimulation with glucose was achieved by addition of 52 mM glucose/KRB into the chamber (final glucose concentration, 22 mM). Diodomethane sulphur immersion oil (Cargille Laboratories) was used to make contact between the objective lens and the coverslip. Measured penetration depths at $\theta = 61.3°$ was about 80 nm [5].

Acquiring the images and analysis

Images were collected by a cooled charge-coupled-device camera (Micromax, MMX-512-BFT, Princeton Instruments; operated with Metamorph 4.6, Universal Imaging). Images were acquired every 50 ms. Most analyses, including tracking (the single projection of different images) and area calculations, were performed using Metamorph software. To analyse the data, fusion events were manually selected, and the average fluorescence intensity of individual granules in a 1 μm × 1 μm square placed over the granule centre was calculated. The number of fusion events was manually counted while looping 15 000 frame time-lapses. Sequences were exported as single TIFF files and further processed using Adobe Photoshop 6.0 or they were converted into QuickTime movies.

Immunohistochemical analysis

Cells were fixed, made permeable with 2 % paraformaldehyde/0.1 % Triton X-100, and processed for immunocytochemistry as described previously [23]. Cells were labelled with monoclonal anti-insulin antibodies (Sigma), then processed with Cy3-conjugated anti-mouse IgG antibody (Amersham Pharmacia Biotech). Immunofluorescence staining was detected with TIRFM.

RESULTS

TIRF imaging analysis of single insulin granules undergoing exocytosis in normal rat primary pancreatic β-cells

Figure 1(A) shows the real-time TIRF images of a single insulin granule motion when stimulated by 22 mM glucose for 15 min in normal rat primary pancreatic β-cells (see Supplemental Movie 1, http://www.BiochemJ.org/bj/381/bj3810013add.htm). The sequential images of single granules obtained every 50 ms revealed a marked difference in exocytotic pathways between the first (0–4 min) and second phase (> 4 min). During the first phase, within the first 240 s after the addition of 22 mM glucose, the fusing granules originated mostly from morphologically previously docked granules, the so-called 'residents' that were visible before glucose stimulation (Figure 1A, resident). As shown in the sequential images of single granules, the fluorescent spot remained nearly constant, as if it were docked to the plasma membrane, then suddenly brightened and vanished within 300 ms. The fusing granules during the second phase arose from 'newcomers', which had been absent or only dimly visible before stimulation, but which probably pre-existed in a reserve pool (Figure 1A, newcomer). It is quite interesting that the newcomer was fused immediately after it reached the plasma membrane. The time from landing to fusion was less than 50 ms.

We then measured the dynamic changes in the number of insulin granules docked to the plasma membrane during the time course of glucose stimulation. The number of previously docked granules decreased, because fusion occurs in previously docked granules during the first phase (Figure 1C, dark grey line), whereas newly recruited granules docked and remained on the cell surface (Figure 1C, light grey line); as a result, the total number of

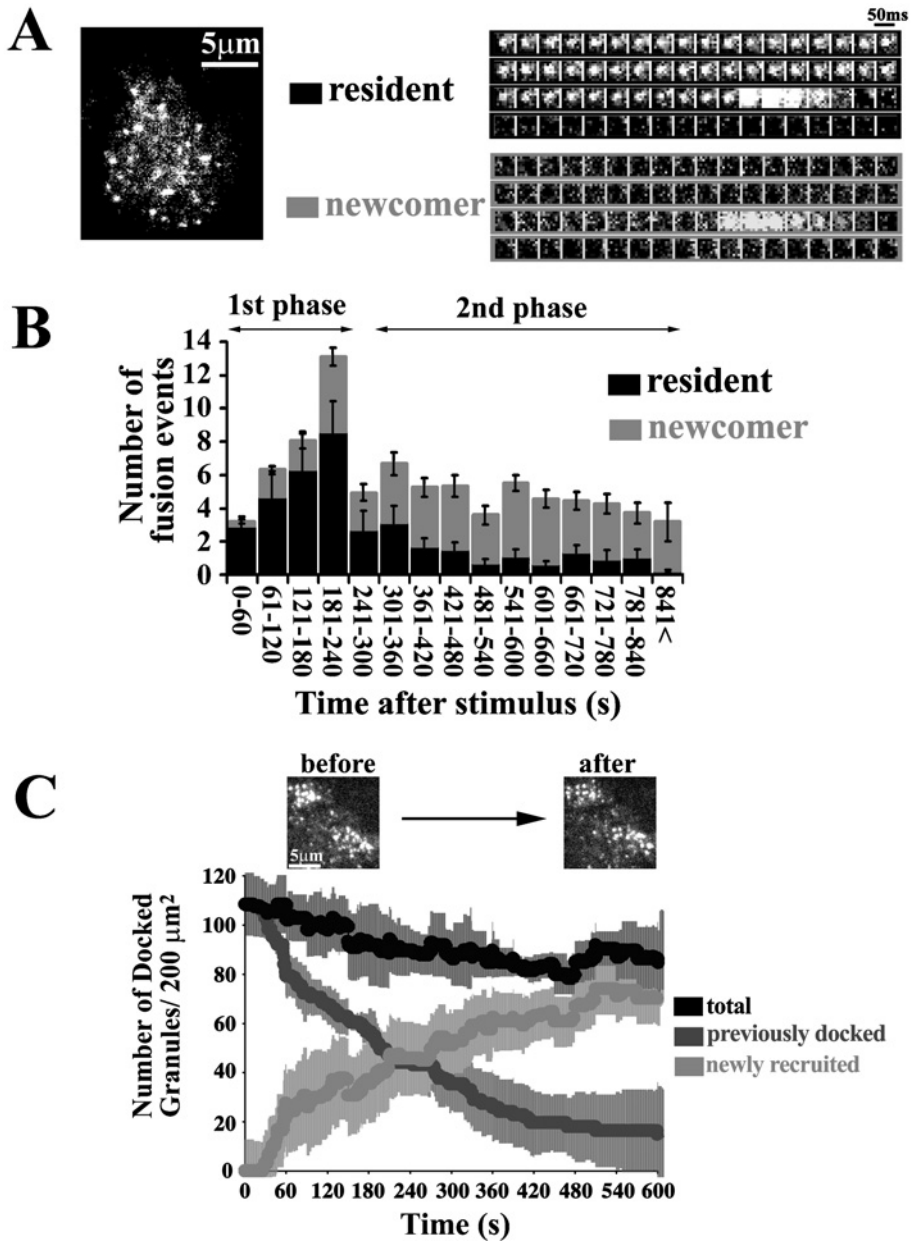

Figure 1 TIRF images and analysis of single GFP-labelled insulin granule motion in normal rat primary β-cells during glucose-induced biphasic insulin release

(**A**) The real-time motion of GFP-labelled insulin granules was imaged close to the plasma membrane (50-ms intervals) (see Supplemental Movie 1, http://www.BiochemJ.org/bj/381/bj3810013add.htm). Sequential images (1 μm $\times$ 1 μm) of a granule docking and fusing with the plasma membrane were presented during stimulation with 22 mM glucose. 'Resident' indicates that the morphologically previously docked granule is fused with the plasma membrane. Fusion is observed as the rapid spread of brightened fluorescence, followed by its disappearance. 'Newcomer' indicates that the granules approach from the inside (being absent before stimulation with 22 mM glucose), reach the plasmalemma and then are quickly fused. (**B**) Histogram showing the number of fusion events (per 200 μm^2) at 60-s intervals after stimulation ($n = 10$ cells). The black columns show the fusion from residents, and the grey columns shows that from newcomers. During the first phase, fusion occurs mostly from residents. The fusing granules during the second phase originate mostly from newcomers. (**C**) Time-dependent change of the number of insulin granules docked to the plasma membrane during glucose stimulation. The number of previously docked granules (dark grey line) and that of newly recruited granules (light grey line) during glucose-stimulation were determined by counting the granules on each sequential image. The black line represents the total number of granules docked to the plasma membrane, which corresponds to the sum of dark and light grey lines in the time course. Time 0 indicate the addition of 22 mM glucose, and the number of docked granules is presented per 200 μm^2.

docked granules, which is the sum of previously docked granules and newly recruited granules (Figure 1C, black line), was only slightly decreased to approx. 80% of the level before glucose stimulation. This finding was apparently different from results in insulinoma MIN6 cells, in which the total number of docked granules increased up to 140% of the initial number after 15 min of glucose stimulation [5].

Docking and fusion of insulin secretory granules in diabetic GK rat β-cells

The docking and fusion process of GFP-tagged insulin granules were imaged in diabetic GK rat β-cells. TIRF images revealed that the fusion from previously docked granules with 22 mM glucose stimulation was rarely observed during the first phase

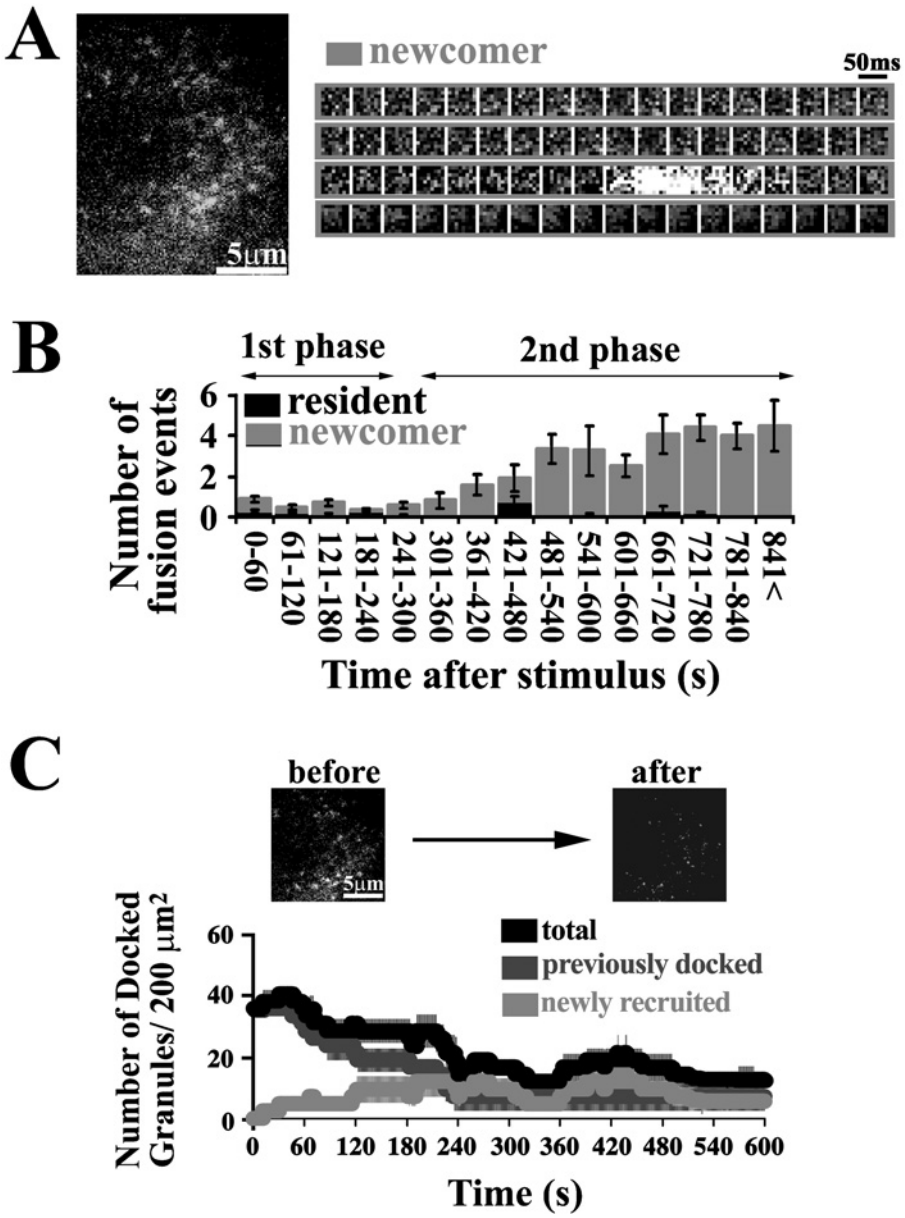

Figure 2 TIRF images and analysis in diabetic β-cells prepared from GK rat pancreas

(**A**) TIRF image during glucose stimulation (see Supplemental Movie 2, http://www.BiochemJ.org/bj/381/bj3810013add.htm) and sequential images of a granule docking and fusing during the second phase. (**B**) Histogram of the number of fusion events (per 200 μm^2) in diabetic β-cells at 60-s intervals after stimulation ($n = 10$ cells). The black and grey columns represent the fusion from residents and newcomers respectively. (**C**) Time-dependent change of the number of docked granules. A line graph shows the dynamic change of docked granules in diabetic β-cells during glucose stimulation as outlined above ($n = 10$ cells).

(see Supplemental Movie 2, http://www.BiochemJ.org/bj/381/bj3810013add.htm), although there were still some previously docked granules observed at the plasma membrane (Figure 2A). The number of fusion events (2.4 ± 0.8 in 0–4 min) during the first phase was markedly reduced in diabetic GK rat β-cells (Figure 2B) compared with that (30.7 ± 2.2 in 0–4 min) in normal β-cells (Figure 1B). On the other hand, no marked differences were observed between normal and diabetic β-cells in the number of fusion events, in particular, during the later second phase (normal, 20.2 ± 1.3 in 10–16 min; diabetic, 19.5 ± 1.2 in 10–16 min). As shown in Figure 2(B), in GK rat β-cells, there was a marked reduction in the fusion from previously docked granules, and, in contrast, fusion from newcomer was almost intact, although the number of fusion events from newcomers slightly decreased. The sequential images of a single insulin granule during the second phase showed that there was not different from that observed in normal β-cells (Figure 2A, right-hand panel).

We then analysed the dynamic changes in the total number of docked granules during glucose stimulation using these TIRF images. In GK rat β-cells, the initial number of GFP-labelled docked insulin granules before glucose stimulation was already reduced (35.7 ± 2.4 versus 108.4 ± 12.9, GK β-cells versus normal β-cells; $P < 0.0001$, $n = 10$ cells). The total number of docked granules in the time course during glucose stimulation remained low, because there was no appreciable number of newly recruited granules to eventually dock to the cell surface and there was

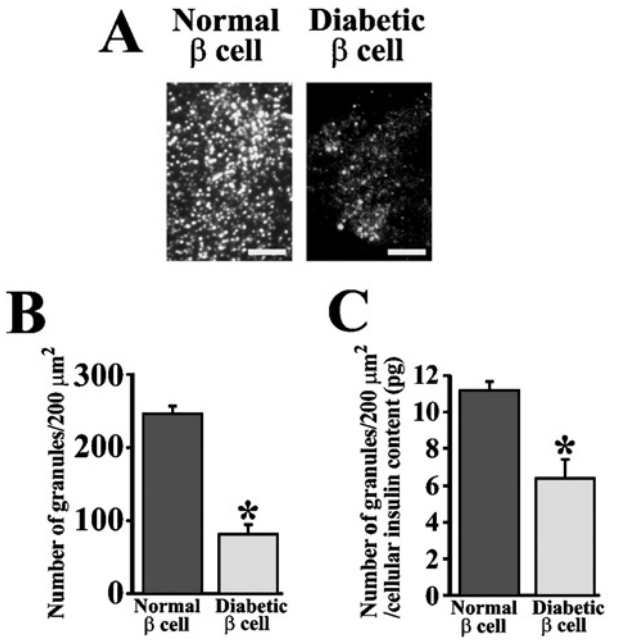

Figure 3 Histochemical study of insulin granules docked to the plasma membrane in normal and diabetic β-cells

(**A**) Endogenous insulin granules in normal and diabetic β-cells imaged by TIRF microscopy. Cells were fixed with paraformaldehyde and then immunostained for insulin. The scale bars represent 5 μm. (**B**) The number of insulin granules morphologically docked to the plasma membrane (per 200 μm^2) in normal and diabetic β-cells by TIRF images ($n = 12$ cells). (**C**) The number of docked granules normalized using cellular insulin content (12.6 ± 2.6 versus 21.7 ± 2.6 pg/cell, GK rat β-cell versus normal cell). The total insulin content in each cell was derived from the total amount of insulin in cultured cells assayed by ELISA, divided by the number of cells and used to normalize the counts. $^*P < 0.0001$ compared with normal β-cells.

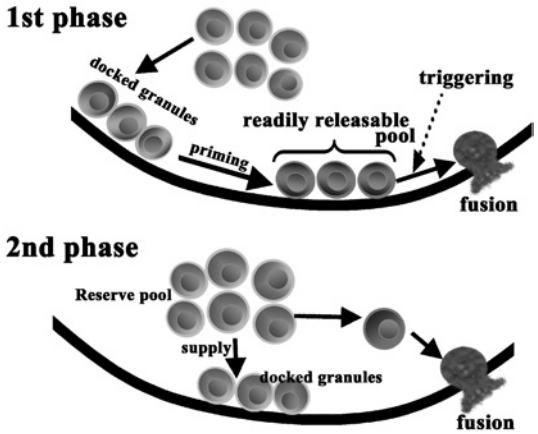

Figure 4 Proposed model for biphasic insulin exocytosis mechanism

During the first phase, some of the previously docked granules are primed by an unknown mechanism and form the RRP. The rise in intracellular [Ca^{2+}] evokes the fusion events from granules in such a pool. During the second phase, the granules jump directly from the reserve pool to the fusion site on the plasma membrane without approaching the RRP and are quickly fused.

an impairment in the cell's ability to retain the already docked granules on the cell surface (Figure 2C). As a result, the total number of docked granules decreased to 35% of initial number after 15 min of glucose stimulation. The finding that fusion from previously docked granules is severely impaired, even though that of newcomers originating from inside the granule pool is still preserved, supports our hypothesis that the insulin exocytotic pathway during the second phase is different from that during the first phase.

Decreased number of endogenous docked insulin granules in diabetic GK rat β-cells observed by TIRFM

Because granules that were fusing mostly originated from previously docked granules during the first phase (Figure 1A), we thought that the total number of endogenous insulin granules docked to the cell surface must decrease in GK β-cells. Therefore we counted the number of docked insulin granules using TIRFM in normal and diabetic β-cells by immunostaining with anti-insulin antibody. Although observing the immunostained insulin granules by epifluorescence microscopy did not allow us to count the individual granules (results not shown), TIRF imaging clearly depicted the single insulin granules morphologically docked to the plasma membrane (Figure 3A), and thus we could count the number of docked insulin granules. As expected, the GK rat β-cells showed a marked decline in the number of docked insulin granules to 33% of normal levels (81 ± 13 granules per 200 μm^2 versus 246 ± 11 per 200 μm^2; $P < 0.0001$, $n = 12$ cells) (Figure 3B). In order to exclude the possibility that this reduction is related to the insulin expression levels, the number of granules was normalized using cellular insulin content (12.6 ± 2.6 versus 21.7 ± 2.6 pg/cell, GK β-cell versus normal cell). The results demonstrated that the number of docked granules was also decreased in GK rat β-cells to 57% of normal levels (Figure 3C), suggesting that this reduction of docked granules was not related to the level of insulin expression.

DISCUSSION

TIRF images of a single insulin granule motion in normal primary β-cells showed that there was a difference in the behaviour of insulin granule motion between insulinoma MIN6 cells and primary pancreatic β-cells. In primary pancreatic β-cells the newcomer was fused immediately after it reached the plasmalemma. In insulinoma MIN6 cells, newcomers remained on the plasma membrane for 66 ± 13 s prior to fusion [5]. Furthermore, there was a distinct difference in the change of the total number of docked granules during glucose stimulation. Thus the dynamics of insulin granule motion near the plasma membrane in primary β-cells is not exactly same as that observed in insulinoma MIN6 cells. The present results in primary β-cells provide new insight into the biphasic insulin exocytotic mechanism: during the second phase, granules from the reserve pool are directly fused without approaching the RRP (readily-releasable pool), and the exocytotic pathway during the second phase does not take the same route of exocytosis as that seen during the first phase (Figure 4).

We analysed the docking and fusion of insulin granules in diabetic GK rat β-cells. Our results demonstrated that in GK rat β-cells: (1) fusion from previously docked granules was almost abolished during first phase, (2) the supply and the ability to retain the granules on the cell surface were impaired, and (3) the number of docked insulin granules decreased, which suggested that the impaired docking followed by fusion plays a role in a loss of insulin exocytosis during the first phase.

It is of interest that the number of docked insulin granules was markedly decreased in diabetic GK rat β-cells to approx. 30% of normal levels. This reduction of docked insulin granules was not due to a decreased insulin content in diabetic β-cells (Figure 3C).

Thus the decrease of docked insulin granules in GK rat β-cell may be one of factors to cause the reduced fusion events during the first phase of insulin release. However, the decreased number of fusion events appears not always to be proportional to the decrease in the number of docked granules, because few fusions were observed during the first phase, despite there being a number of docked granules remaining on the cell surface. This observation suggests that a reduction in fusion events results from not only the decreased number of docked granules, but also probably from impairments to the priming step [25] from docking to fusion; in other words, the process of unprimed docked granules becoming primed docked granules (RRP) or that from RRP to fusion must be disturbed in diabetic β-cells.

In conclusion, we present direct evidence that there is an impaired docking and fusion of insulin granules in diabetic β-cells, which contributes to the loss of first-phase insulin release.

We thank Dr I. Saito (Laboratory of Molecular Genetics, Institute of Medical Science, University of Tokyo, Japan) for the gift of adenovirus cosmid vector and parental virus. This work was supported by Grants-in-Aid for Scientific Research (C) 14570130 (to M. O.-I.), (B) 15390108 (to S. N.), Scientific Research on Priority Areas 16044240 (to M. O.-I.), and Exploratory Research 14657043 (to S. N.) from the Japanese Ministry of Education, Culture, Sports, Science and Technology, and by a grant from Japan Private School Promotion Foundation (to S. N.).

REFERENCES

1 Lang, T., Wacker, I., Steyer, J., Kaether, C., Wunderlich, I., Soldati, T., Gerdes, H. H. and Almers, W. (1997) Ca^{2+}-triggered peptide secretion in single cells imaged with green fluorescent protein and evanescent wave microscopy. Neuron **18**, 857–863

2 Rohrbach, A. (2000) Observing secretory granules with a multi-angle evanescent wave microscopy. Biophys. J. **78**, 2641–2654

3 Johns, L. M., Levitan, E. S., Shelden, E. A., Holz, R. W. and Axelrod, D. (2001) Restriction of secretory granule motion near the plasma membrane of chromaffin cells. J. Cell Biol. **183**, 177–190

4 Axelrod, D. (2001) Total internal reflection fluorescent microscopy in cell biology. Traffic **2**, 764–774

5 Ohara-Imaizumi, M., Nakamichi, Y., Tanaka, T., Ishida, H. and Nagamatsu, S. (2002) Imaging exocytosis of single insulin secretory granules with evanescent wave microscopy. J. Biol. Chem. **277**, 3805–3808

6 Efendic, S. and Ostenson, C.-G. (1993) Hormonal responses and future treatment in non-insulin-dependent diabetes mellitus. J. Intern. Med. **234**, 127–138

7 Ward, W. K., Bolgiano, D. C., McKnight, B., Halter, J. B. and Porte, Jr, D. (1984) Diminished β-cell secretory capacity in patients with non-insulin-dependent diabetes mellitus. J. Clin. Invest. **74**, 1318–1328

8 O'Rahilly, S. P., Nugent, Z., Rudenski, A. S., Hosker, J. P., Burnett, M. A., Darling, P. and Turner, R. C. (1986) Beta-cell dysfunction rather than insulin insensitivity is the primary defect in familial type 2 diabetics. Lancet **11**, 360–364

9 Ashcroft, F. and Rorsman P. (1989) Electrophysiology of the pancreatic β cell. Prog. Biophys. Mol. Biol. **54**, 87–143

10 Wollheim, C. B., Lang, J. and Regazzi, R. (1996) The exocytotic process of insulin secretion and its regulation by Ca^{2+} and G-proteins. Diabetes Rev. **4**, 276–297

11 Hughes, S. J., Faehling, M., Thorneley, C. W., Proks, P., Ashcroft, F. M. and Smith, P. A. (1998) Electrophysiological and metabolic characterization of single beta-cells and islets from diabetic GK rats. Diabetes **47**, 73–81

12 Kato, S., Ishida, H., Tsuura, Y., Tsuji, K., Nishimura, M., Horie, M., Taminato, T., Ikehara, S., Okada, H., Ikeda, H., Okada, Y. and Seino, Y. (1996) Alterations in basal and glucose stimulated voltage-dependent calcium channel activities in pancreatic beta cells of NIDDM GK rats. J. Clin. Invest. **97**, 2417–2425

13 Portha, B., Giroix, M. H., Serradas, P., Welsh, N., Hellerstrom, C., Sener, A. and Malaisse, W. J. (1988) Insulin production and glucose metabolism in isolated pancreatic islets of rats with NIDDM. Diabetes **37**, 1226–1233

14 Ostenson, C. G., Khan, A., Abdel-Halim, S. M., Guenifi, A., Suzuki, K., Goto, Y. and Efendic, S. (1993) Abnormal insulin secretion and glucose metabolism in pancreatic islets from the spontaneously diabetic GK rat. Diabetologia **36**, 3–8

15 Giroix, M. H., Vesco, L. and Portha, B. (1993) Functional and metabolic perturbations in isolated pancreatic islets from the GK rat, a genetic model of non-insulin-dependent diabetes. Endocrinology **132**, 815–822

16 Zong-Chao, L., Efendic, S., Wibom, R., Abdel-Halim, S. M., Ostenson, C. G., Landau, B. R. and Khan, A. (1998) Glucose metabolism in Goto–Kakizaki rat islets. Endocrinology **139**, 2670–2675

17 Sudhof, T. C. (1995) The synaptic vesicle cycle: a cascade of protein–protein interactions. Nature (London) **375**, 645–653

18 Nagamatsu, S., Fujiwara, T., Nakamichi, Y., Watanabe, T., Katahira, H., Sawa, H. and Akagawa, K. (1996) Expression and functional role of syntaxin 1/HPC-1 in pancreatic β cells. J. Biol. Chem. **271**, 1160–1165

19 Wheeler, M. B., Sheu, L., Ghai, M., Bouquillon, A., Grondin, G., Weller, U., Beaudoin, A. R., Bennett, M. K., Trimble, W. S. and Gaisano, H. Y. (1996) Characterization of SNARE protein expression in β cell lines and pancreatic islets. Endocrinology **137**, 1340–1348

20 Nagamatsu, S., Nakamichi, Y., Yamamura, C., Matsushima, S., Watanabe, T., Ozawa, S., Furukawa, H. and Ishida, H. (1999) Decreased expression of t-SNARE, syntaxin 1, and SNAP-25 in pancreatic beta-cells is involved in impaired insulin secretion from diabetic GK rat islets: restoration of decreased t-SNARE proteins improves impaired insulin secretion. Diabetes **48**, 2367–2373

21 Gaisano, H. Y., Ostenson, C. G., Sheu, L., Wheeler, M. B. and Efendic, S. (2002) Abnormal expression of pancreatic islet exocytotic soluble *N*-ethylmaleimide-sensitive factor attachment protein receptors in Goto–Kakizaki rats is partially restored by phlorizin treatment and accentuated by high glucose treatment. Endocrinology **143**, 4218–4226

22 Zhang, W., Khan, A., Ostenson, C. G., Berggren, P. O., Efendic, S. and Meister, B. (2002) Down-regulated expression of exocytotic proteins in pancreatic islets of diabetic GK rats. Biochem. Biophys. Res. Commun. **291**, 1038–1044

23 Nagamatsu, S., Watanabe, T., Nakamichi, Y., Yamamura, C., Tsuzuki, K. and Matsushima, S. (1999) α-Soluble *N*-ethylmaleimide-sensitive factor attachment protein is expressed in pancreatic β-cells and functions in insulin, but not γ-amino butyric acid secretion. J. Biol. Chem. **274**, 8053–8060

24 Pouli, A. E., Kennedy, H. J., Schofield, J. G. and Rutter, G. A. (1998) Insulin targeting to the regulated secretory pathway after fusion with green fluorescent protein and firefly luciferase. Biochem. J. **331**, 669–675

25 Eliasson, L., Renstrom, E., Ding, W. G., Proks, P. and Rorsman, P. (1997) Rapid ATP-dependent priming of secretory granules precedes Ca^{2+}-induced exocytosis in mouse pancreatic β-cells. J. Physiol. (London) **503**, 399–412

Received 16 March 2004/4 May 2004; accepted 5 May 2004
Published as BJ Immediate Publication 6 May 2004, DOI 10.1042/BJ20040434